AD-A129 138 FIBER OPTIC ELECTRIC FIELD SENSOR INVESTIGATIONS II(U) 1/
TRACOR INC ROCKVILLE MD M D MERMELSTEIN 02 MAY 83
TRACOR-T-83-RV-5260 N00014-81-C-0515

UNCLASSIFIED F/G 17/8 NL

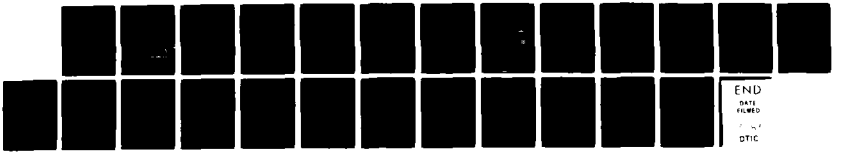

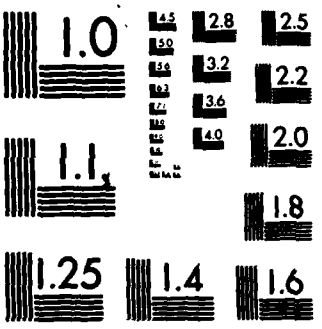

MICROCOPY RESOLUTION TEST CHART
NATIONAL BUREAU OF STANDARDS-1963-A

Tracor Document No. T-83-RV-5260 (U)
Tracor Contract No. N0014-81-C-0515

FINAL REPORT

FIBER OPTIC ELECTRIC FIELD SENSOR INVESTIGATIONS, II

Submitted to:

Department of the Navy
Office of Naval Research
800 N. Quincy Street
Arlington, VA 22217

ATTN: Dr. D. Polk, Code 431

2 May 1983

Tracor Applied Sciences

Tracor, Inc.
1601 Research Blvd.
Rockville, Maryland 20850
Telephone 301·279-4200

Tracor Document No.: T-83-RV-5260 (U)
Tracor Contract No.: N0014-81-C-0515

FIBER OPTIC ELECTRIC FIELD SENSOR INVESTIGATIONS, II

Submitted to:

Department of the Navy
Office of Naval Research
800 N. Quincy Street
Arlington, VA 22217

Attn: Dr. D. Polk, Code 431

2 May 1983

Approved by:

Wentworth Williams, Jr.
Branch Manager
Applied Sciences Group

Prepared by:

Marc D. Mermelstein
Senior Scientist

TABLE OF CONTENTS

LIST OF ILLUSTRATIONS

LIST OF TABLES

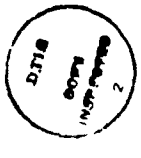

1.0 INTRODUCTION

In June 1981 the Office of Naval Research contracted with Tracor, Inc. to experimentally investigate the potential of interfacing piezoelectric polymers and single mode fibers for the development of an optical fiber electric field sensor. Results of the first portion of these investigations appeared in the Annual Report entitled "Fiber Optic Electric Field Sensor Investigations," dated September 20, 1982.

The continuation and conclusion of that effort is reported herein. Experiments were performed in Tracor's Optics Laboratory whereby a single mode fiber was embedded in a piezoelectrically active vinylidene fluoride-tetrafluoroethylene copolymer film. Application of an external electric field to the fiber copolymer composite induces strains in the polymer film that are transferred to the core of the optical fiber. The resultant phase shift in the propagating light is detected with a Mach-Zehnder interferometer and correlated to the amplitude of the applied electric field.

Section 2.0 of this report briefly discusses fiber optic sensors and reviews published results for fiber optic electric field detectors. Section 3.0 describes the device fabrication including the poling procedure used to induce piezoelectric activity in the copolymer film and the technique by which the copolymer piezoelectric constant was measured. The interferometric measurements are described in section 4.0 together with the experimental results. Section 5.0 presents an analysis of the experimental data. This analysis includes a model prediction for the static electric field detection sensitivity, an identification of the device resonant mode structure, and a determination of the local electric field strength in the copolymer film. A summary of the highlights of this experimental program is given in section 6.0 along with recommendations for the optimization of the device performance.

2.0 BACKGROUND

Fiber optic sensors have undergone intensive development over the past few years. These sensors have been used for the detection and measurement of a variety of physical quantities including acoustic pressure, hydrostatic pressure, temperature, magnetic, and electric field strengths. Fiber optic sensors can be divided into two distinct categories-phase sensitive detectors and intensity sensitive detectors. Phase sensitive sensors utilize single-mode fibers in a Mach-Zehnder interferometric configuration. The detected field induces a change in the optical path length of one arm of the interferometer. The optical output of the sensing arm is then mixed with the output of a reference arm to produce a phase sensitive optical signal. The phase is linearly proportional to the detected field.

Considerable effort has been directed towards integrating piezoelectric polymers and single mode fibers in the development of an electric field sensor. Corome and Koo[1] first demonstrated that the optical phase of light propagating in a bare single mode fiber that is attached to the external surface of oriented and electroded poly(vinylidene-fluoride), PVDF, films can be modulated by an applied voltage. This device was investigated further by Koo and Sigel.[2] Donalds et al.[3] have jacketed a single mode fiber with an unspecified material, poled the jacket, and measured an electric field induced optical phase shift. Described here is a fiber optic electric field detector consisting of a single mode fiber embedded in a poled vinylidene fluoride and tetrafluoroethylene, P(VDF-TFE), copolymer film. This device is a self-contained detector in which the copolymer film serves the dual function of protecting the optical waveguide and providing the piezoelectric activity.

3.0 DEVICE FABRICATION

3.1 Fiber-Copolymer Composite

A 73 wt percent vinylidene fluoride and 27 wt percent tetrafluoroethylene copolymer was obtained in pellet form from the Pennwalt Corporation.[4] P(VDF-TFE) solidifies from the melt in the β phase and can be subsequently poled at moderate electric field strengths without mechanical orientation. The pellets were placed between two sheets of aluminum foil and pressed into ~200 μm films by plattens heated to a temperature just below the copolymer melt temperature of 126°C. The aluminum foil was then removed from the copolymer films. A bared segment of fiber was sandwiched by two such films which were then pressed into a single film. Contact electrodes having a 2 cm width were placed on the surface of the copolymer above the optical fiber. The electroded fiber-copolymer composite was immersed in a 70°C dielectric oil bath and a poling electric field of approximately 325 kV/cm was applied. The poling field was maintained as the oil bath temperature was reduced to room temperature in ten minutes. This fabrication procedure is illustrated in Figure 1.

3.2 Measurement of the d_{33} Piezoelectric Coefficient

Films without fibers were poled in an identical manner and placed in a hydraulic press. A pressure p_0 was applied to the film surfaces, as illustrated in Figure 2, and then quickly relieved. The resultant voltage drop across the input impedance of an oscilloscope was monitored. It is possible to relate the d_{33} piezoelectric modulus to the area under the voltage trace appearing on the oscilloscope. The piezoelectric polymer film is characterized by the following constitutive equation:

$$P_3 = \chi_{33} E_3 + d_{33} \sigma_{33} \qquad (1)$$

where P_3 is the polarization, χ_{33} is the dielectric susceptibility, E_3 the electric field, and σ_{33} the stress. The current density J_3 flowing through

MANUFACTURING OF THICK FILMS FROM P(VDF-TFE) PELLETS; PENWALT KYNER: 7200

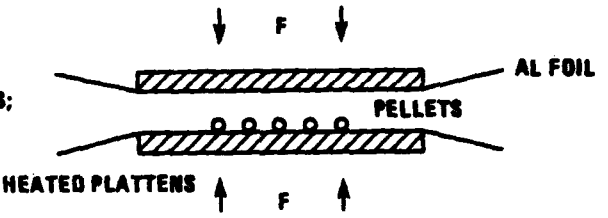

SANDWICHING FIBER WITH TWO SUCH FILMS AND UNIFYING WITH HEATED PLATTENS

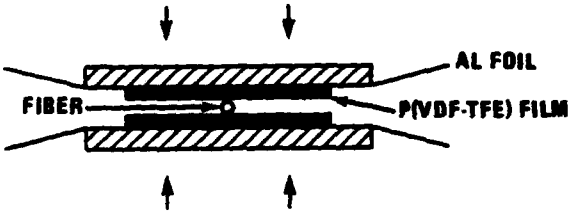

POLING IN OIL BATH AT 70° C AND FIELD OF 300kV/CM. TEMP REDUCED TO 25° C WITHIN 10 MINUTES WITH VOLTAGE ON

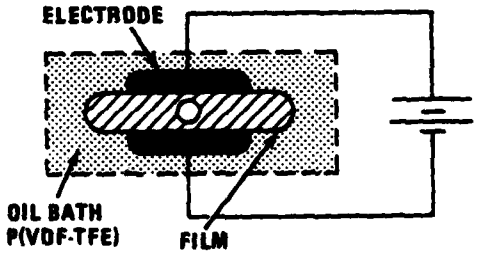

INTERFACING OF FIBER AND COPOLYMER

FIG.1. Fabrication steps followed to embed the single mode fiber in the copolymer film and the poling apparatus.

MEASURED d_{33} PIEZOELECTRIC COEFFICIENT IN FIBER-FREE FILM USING HYDRAULIC PRESS

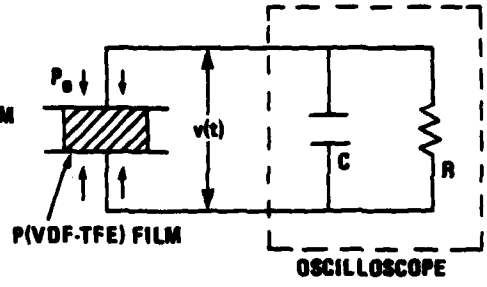

$$d_{33} = \frac{-1}{RAp_0} \int_i^f dt\, v(t)$$

$$d_{33} = -5.7 \times 10^{-12}\ m/V$$

FIG. 2. Technique for measuring the d_{33} piezoelectric modulus in copolymer film.

the polymer is

$$J_3 = \frac{1}{\rho}E_3 + \frac{1}{4\pi}\frac{\partial D_3}{\partial t} \tag{2}$$

where ρ is the polymer resistivity and D_3 the electric displacement defined by

$$D_3 = E_3 + 4\pi P_3 \ . \tag{3}$$

Substitution of eq. (1) for the polarizations yields the following equation for the electric displacement D_3

$$D_3 = \epsilon_{33}E_3 + 4\pi d_{33}\sigma_{33} \tag{4}$$

and dielectric constant ϵ_{33}

$$\epsilon_{33} = 1 + 4\pi\chi_{33} \ . \tag{5}$$

Assuming that the dielectric constant ϵ_{33} and the piezoelectric modulus d_{33} are not time dependent, then the current density becomes

$$J_3 = \frac{1}{\rho}E_3 + \frac{\epsilon_{33}}{4\pi}\frac{\partial E_3}{\partial t} + d_{33}\frac{\partial \sigma_{33}}{\partial t} \ . \tag{6}$$

The requirement that the current leaving the polymer film must be equal to the current flowing into the oscilloscope impedance yields the following differential equation for the voltage across the polymer:

$$\frac{A_{el}}{\rho}\frac{V}{L} + \frac{\epsilon A_{el}}{4\pi}\frac{\partial E_3}{\partial t} + A_{el}\, d_{33}\frac{\partial \sigma_{33}}{\partial t} = \frac{-V}{R} - C\frac{\partial V}{\partial t} \tag{7}$$

where

A_{el} - polymer electrode area
V - voltage across polymer
L - thickness of polymer fiber
R - oscilloscope resistance
C - oscilloscope capacitance .

Integration of (7) gives:

$$\frac{A_{el}}{\rho L}\int_0^{\infty} dt\ V(t) + \frac{\epsilon_{33} A_{el}}{4\pi}\left[E(\infty) - E(o)\right]$$

$$+ A_{el}\ d_{33}\ \left[\sigma_{33}(\infty) - \sigma_{33}(o)\right] = \frac{-1}{R}\int_0^{\infty} dt\ V(t)$$

$$-C\left[V(\infty) - V(o)\right] . \qquad (8)$$

Application of the appropriate boundary conditions for the initial and final states in (8) then gives the following expression for the d_{33} piezoelectric modulus:

$$d_{33} = \frac{-1}{R_{tot}}\ A_{el}\ P_o \int_0^{\infty} dt\ V(t) \qquad (9)$$

where $$\frac{1}{R_{tot}} = \frac{1}{R} + \frac{A_{el}}{\rho L} . \qquad (10).$$

This measurement procedure was calibrated against a standard polymer provided by the manufacturer. Figure 3 plots the measured d_{33} piezoelectric modulus as a function of time. It is seen that d_{33} falls from an initial value of -7.6 pC/N to a value of -5.7 pC/N after five days. It remains relatively stable thereafter.

4.0 INTERFEROMETRIC MEASUREMENTS

The fiber optic electric field sensor is illustrated in Figure 4. The sample, whose characteristics are presented here, has a mean thickness of 212 μm and an activated length of 12 cm. The fiber outside diameter and core diameter are 100 μm and 4 μm, respectively. An oscillating electric field was applied to the sensor by capacitor plates with a 2 mm spacing. The electric field causes the piezoelectric polymer to strain. Fluctuations

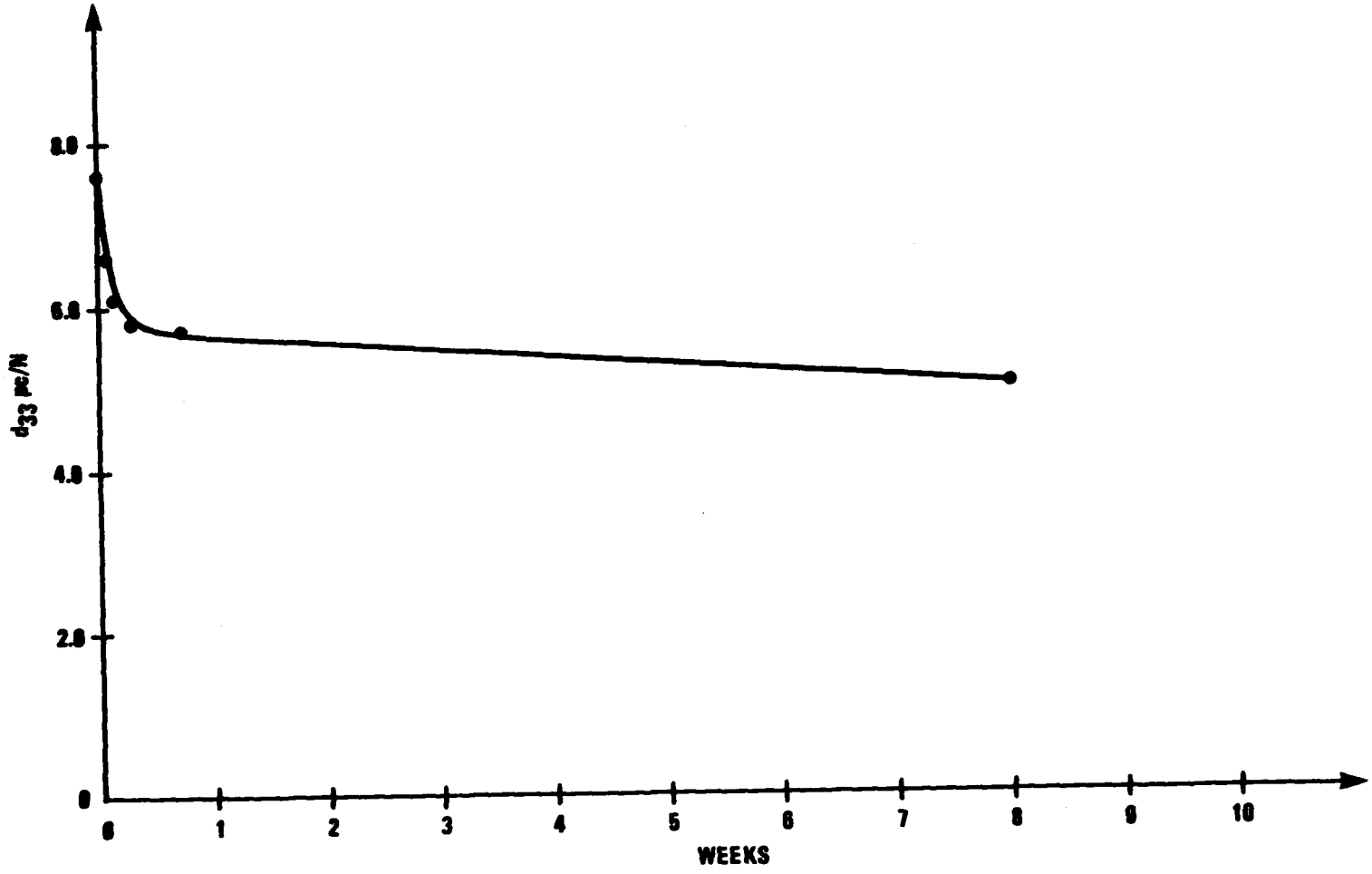

FIG. 3. Plot of measured d_{33} piezoelectric modulus in copolymer film as a function of time.

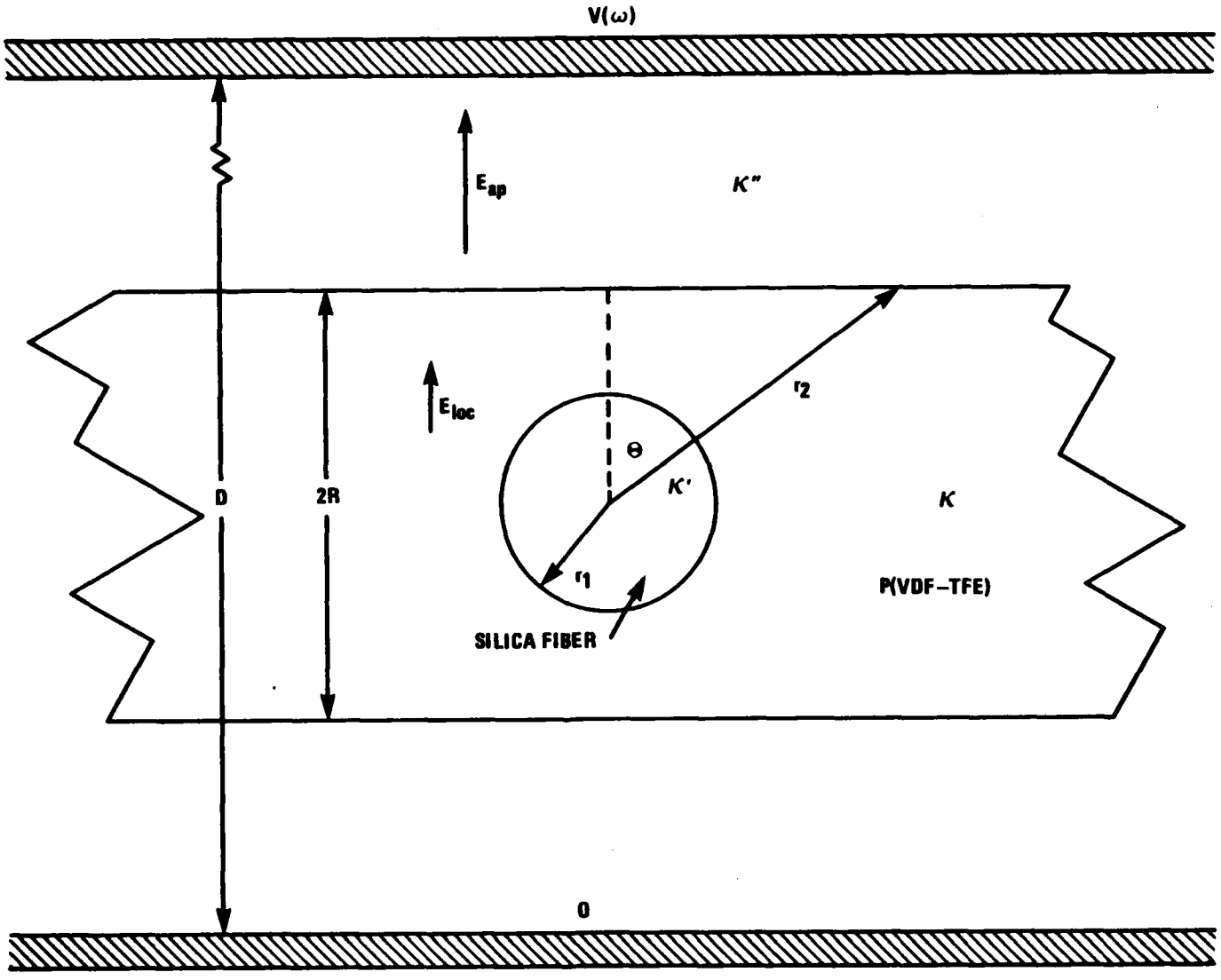

FIG. 4. Illustration of fiber-copolymer field detector and electric fields generated by the capacitor plates.

of the strain in the polymer are transmitted to the fiber core and induce fluctuations in the optical path length, thereby modulating the phase of the propagating wave.

The fiber optic interferometer, electric field sensor, and associated electronics are shown in Figure 5. Light from a He-Ne laser is divided by a beam splitter and focused into the cores of the single mode fibers by X10 microscope objectives. The outputs of the reference and sensing arms are recombined at the second beam splitter. Light from the center of the resultant ring pattern is collected by a lens and focused onto the surface of a silicon detector, producing a photocurrent proportional to the irradiance. The irradiance exiting either arm of the interferometer is determined (to within a proportionality factor) by measuring the voltage drop across a loading resistor R'_L. Fluctuations in the combined beam irradiance, resulting from the applied electric field are given by:

$$\delta I(t) = -2\sqrt{I_1 I_2}\,|\gamma_{12}|\left[(\delta\psi_s)\sin\psi_0 + \frac{1}{2}(\delta\psi_s)^2\cos\psi_0 - \frac{1}{6}(\delta\psi_s)^3\sin\psi_0 + \ldots\right] \tag{11}$$

where δI is the combined beam irradiance fluctuations, I_1 and I_2 are the irradiance exiting the respective arms of the interferometer, and γ_{12} is the degree of partial coherence of the laser light. The phase difference between the two interferometer arms for zero electric field is ψ_0 and the field-induced phase fluctuations are $\delta\psi_s$. In equation (9) it has been assumed that $\delta\psi_s \ll 1$. For an applied electric field $\delta E_{ap}(\omega_0)$ oscillating at a frequency ω_0, the amplitude of the field-induced fluctuating phase is related to the total power (in units of volts squared) at ω_0 by

$$\Delta\psi_s = \frac{R'_L}{R_L G}\,\frac{1}{|\gamma_{12}|}\sqrt{\frac{\langle P_{\omega_0}\rangle}{v_1(0)\,v_2(0)}} \tag{12}$$

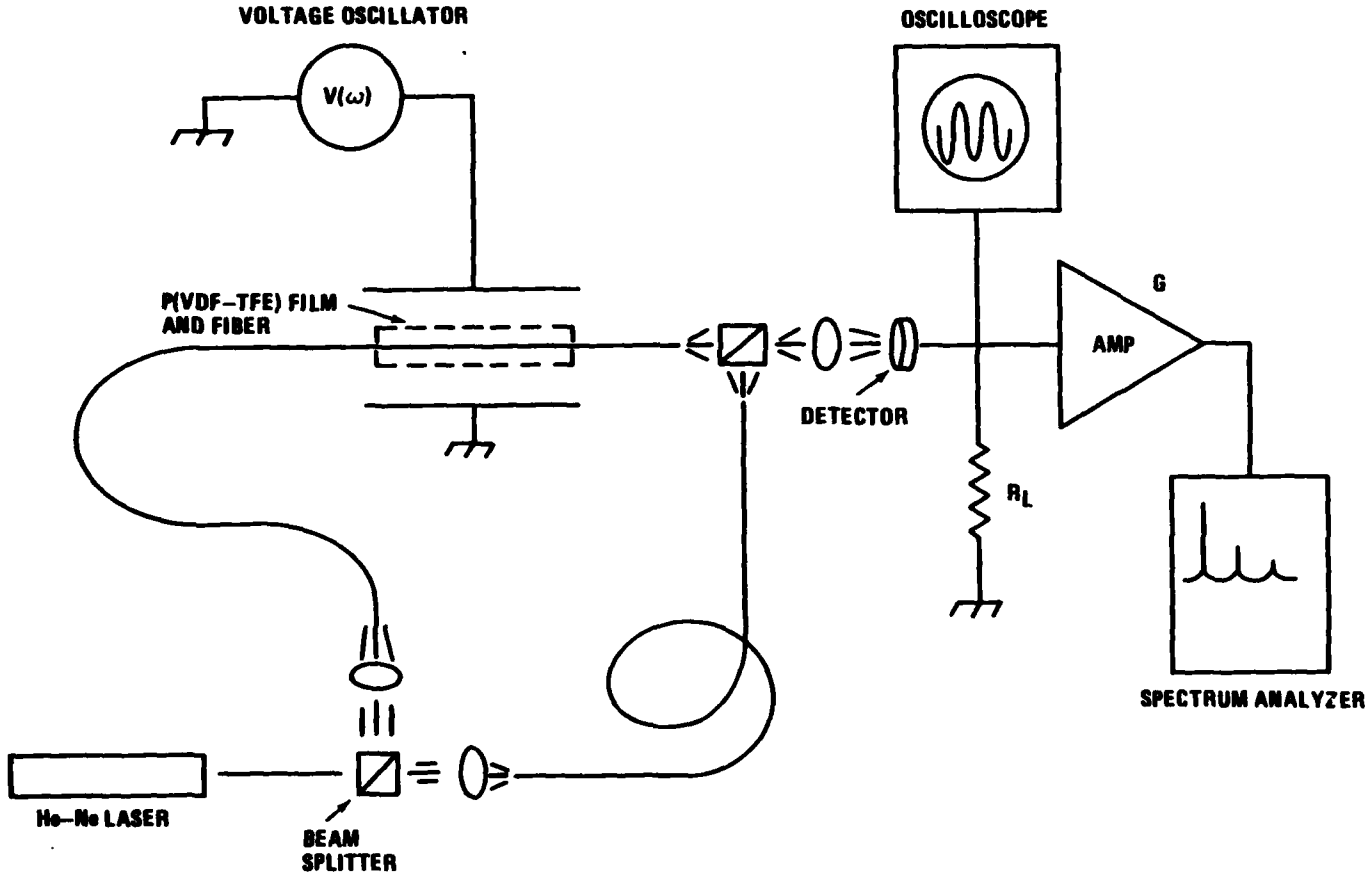

FIG. 5. Fiber optic Mach-Zehnder interferometer with field detector incorporated as the sensing arm. Also shown are the associated signal processing electronics.

where G is the gain of the amplifier, $\langle P_{\omega_0} \rangle$ represents an averaged value for the total power at ω_0 resulting from a large number of measurements and $v_1(0)$ and $v_2(0)$ are the voltages associated with the irradiances in the respective arms of the interferometer. Equation (12) applies to an unstabilized interferometer that randomly drifts in and out of quadrature. The total power at the fundamental frequency was measured with the spectrum analyzer. Plotted in Figure 6 are the measured phase shift amplitudes $\Delta\psi_s$, from Eq. (12), as a function of the applied field strength amplitude E_{ap} at 5.0 kHz. The error bars are primarily due to drift in the optical alignment during the course of the measurement. The linear dependence of the phase shift amplitude on the applied field strength (within experimental error) is clearly evident.

The intrinsic detector sensitivity is defined in the frequency domain by

$$\eta(\omega) = \frac{\delta\psi_s(\omega)}{\langle\psi_s(t)\rangle_t \delta E_{ap}(\omega)} \tag{13}$$

where $\langle\psi_s\rangle_t$ is the time averaged phase change after traversal of the detector length. The sensitivity $\eta(\omega)$ of the detector was determined in the frequency region of 1.0 kHz to 100 kHz by varying the frequency of a constant amplitude applied field strength and measuring the resultant phase shift amplitude. These results are presented in Figure 7. Power spectra below 1.0 kHz were not readily accessible due to the presence of significant low frequency noise in the unstabilized interferometer. At 1.0 kHz the sensor exhibits a sensitivity of $(0.20 \pm 0.03) \times 10^{-12}$ m/V. Note that η has units of the piezoelectric modulus and is a measure of the core strain in response to the field. There are two apparent peaks in the frequency response, one at approximately 3.5 kHz and a stronger peak at approximately 14 kHz. Furthermore, there is a steady rise in $\eta(\omega)$ as the frequency approaches 100 kHz suggesting the presence of a third peak that is outside the frequency range. These peaks are tentatively identified as the mechanical resonant structure of the fiber-copolymer composite. More will be said concerning this frequency structure in section 5.3.

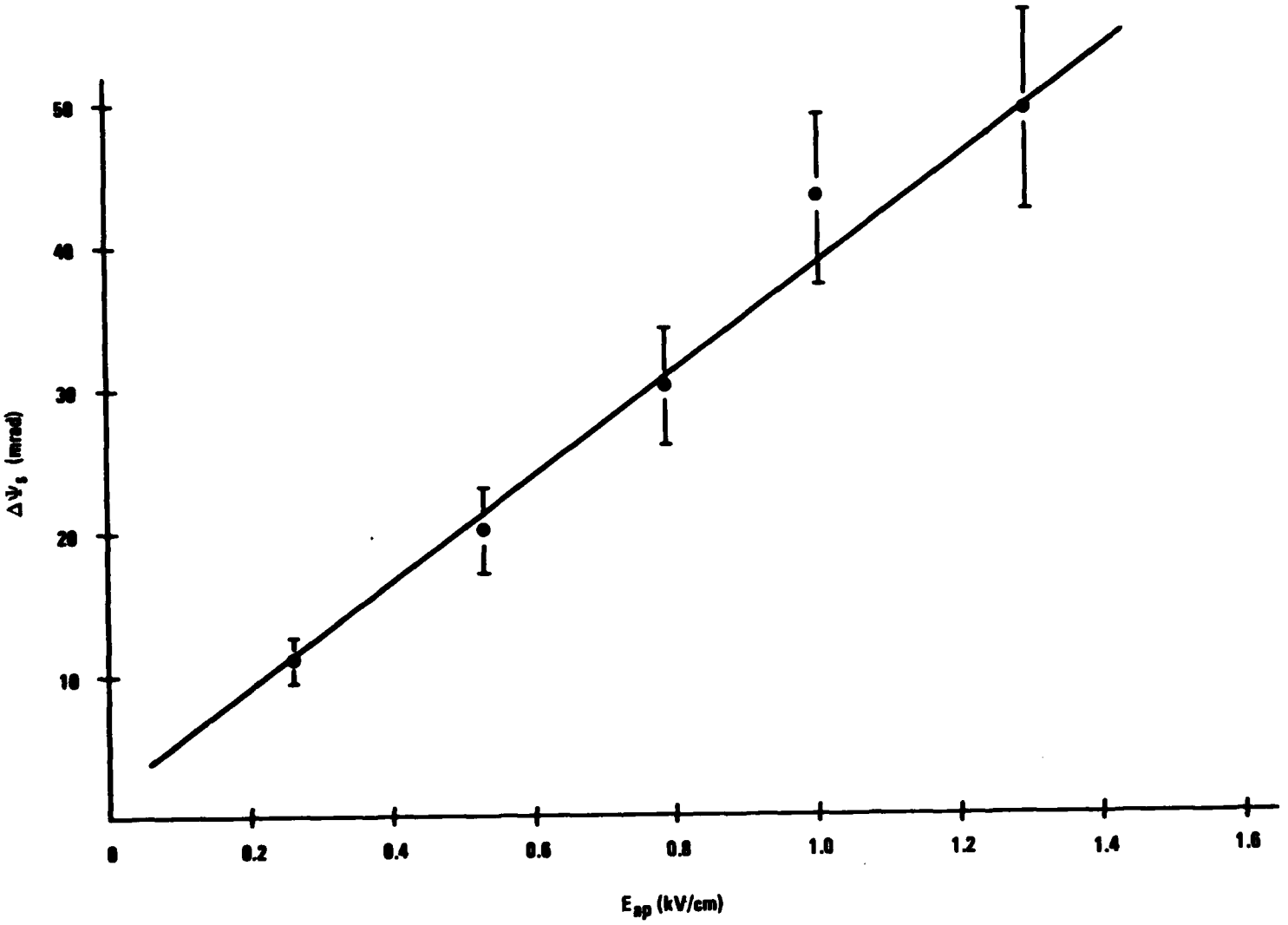

FIG. 6. Shown are the measured phase shift amplitudes verifying amplitude response linearity.

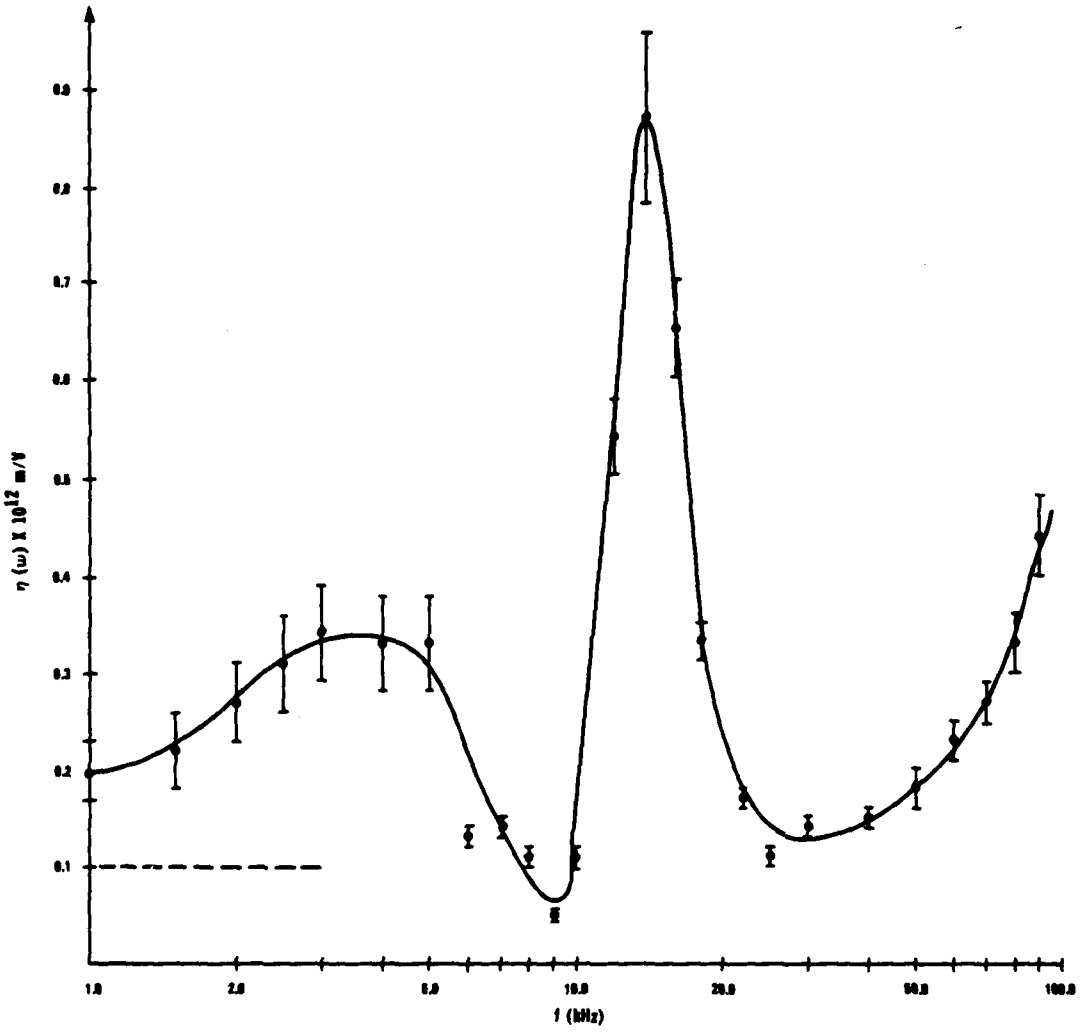

FIG. 7. Intrinsic sensitivity $\eta(\omega)$ as a function of frequency of a constant amplitude, sinusoidal applied electric field. Peaks presumably arise from the resonant structure of the fiber-copolymer composite. The solid line is drawn as a guide to the eye. Dotted line is static prediction of equation (18).

5.0 ANALYSIS AND INTERPRETATION

5.1 Sensitivity Analysis

DeSouza and Mermelstein[5] have obtained a model expression for the static sensitivity $\eta(o)$ of a single mode fiber of radius r_1 clad in a cylindrical piezoelectric polymer jacket of radius r_2 which has been poled in the direction normal to the fiber axis. The static sensitivity as a function of material and geometric parameters is:

$$\eta(o) = \eta_{max}\, f(r_1, r_2) \tag{14}$$

where the maximum sensitivity is

$$\eta_{max} = \frac{1}{N}\left\{ 1 - \frac{1}{2}n^2 \left[(P_{11} - 2P_{44}) + \frac{\sigma'}{\sigma - 1} (P_{11} - P_{44}) \right] \right\} d^{eff} \tag{15}$$

and the structure factor f is

$$f(r_1, r_2) = \frac{1}{1 + \frac{\mu\sigma(1-\sigma')}{\mu'\sigma'(1-\sigma)} \left[\frac{r_2^2}{r_1^2} - 1 \right]^{-1}} \cdot \tag{16}$$

The effective piezoelectric modulus d^{eff} is defined by

$$d^{eff} = d_{31} + \frac{d_{32} + d_{33}}{2\sigma} \tag{17}$$

and N relates the applied electric field to the local field inside the copolymer: $E_{loc} = E_{ap}/N$. All quantities in equations (15), (16), and (17) are tabulated in Table I. The structure factor f may be adapted to the planar geometry employed here by taking a suitable average. Hence, for the planar sensor, the sensitivity is

$$\eta(o) = \eta_{max}\, g(r_1, R) \tag{18}$$

Table 1. Material Parameters Used in Fiber Optic Electric Field Sensor Sensitivity Calculation.

Material	Parameter	Value	Ref
Silica	Lame parameter μ'	3.1×10^{11} dynes/cm^2	6
	Poisson's ratio σ'	0.17	6
	Pockel's Coefficients:		
	p_{11}	0.125	7
	p_{44}	-0.072	7
	Refractive index n at $\lambda = 0.63$ μm	1.46	6
	dielectric constant κ'	3.78	6
P(VDF-TFE)	Lamé parameter μ	3.6×10^9 dynes/cm^2	8
	Poisson's ratio σ	-0.4	8
	dielectric constant κ	7.2	8
PVDF-biaxially Oriented film	Piezoelectric moduli:		
	d_{33}	-12.4×10^{-12} m/V	9
	d^{eff}	-5.7×10^{-12} m/V	9
	dielectric constant	13	10

where

$$g(r_1, R) = \frac{2}{\pi} \int_0^{\pi/2} d\Phi \; f\,(r_1, R \sec \Phi). \tag{19}$$

Hence, an estimate for the zero frequency electric field detection sensitivity has been obtained in terms of the fiber and copolymer material and geometric parameters.

The determination of the local field distribution in the neighborhood of the fiber is complex. As an approximation, it will be assumed that the local field is everywhere parallel to the applied field and that the depolarization coefficient N is equal to its value for a dielectric slab immersed in a uniform field set up by capacitor plates with spacing D:

$$N = \frac{K}{K''} - \left(\frac{K}{K''} - 1 \right) \frac{2R}{D} \tag{20}$$

Here K is the dielectric constant of the copolymer and K'' is the dielectric constant of the surrounding media.

The effective piezoelectric modulus for the copolymer is estimated by multiplying d^{eff} for PVDF by $d_{33}(\text{VDF-TFE})/d_{33}(\text{PVDF})$. Equations (15), (18), (19) and (20) along with the appropriate values for the material parameters and device geometry yield a predicted static sensitivity of 0.10×10^{-12} m/V. Figure 7 indicates that $\eta(\omega)$ is decreasing as the frequency approaches 1.0 kHz from above. Assuming that the peak at 3.5 kHz represents a mechanical resonance and that there are no other significant resonances below 1.0 kHz, it is reasonable to expect that the sensitivity will continue to decrease, as the frequency approaches zero, approaching a value consistent with the static analysis. A direct verification of the theoretical prediction will require sensitivity measurements in the very low frequency region.

5.2 Depolarization Field

If an electric field is applied to a dielectric slab immersed in a medium of a differing dielectric constant, then a surface charge density develops at the interfaces. This surface charge density contributes to the local field inside the dielectric slab. The ratio of the applied field to local field is N which is given by equation (20). The field-induced strain in a piezoelectric material is proportional to the local electric field. Hence, the sensitivity of the fiber optic electric field sensor will be dependent upon the dielectric constants of the polymer and external medium. This dependence was tested by repeating the sensitivity measurements with the field sensor and capacitor plates (3 mm spacing) placed in a bath of glycerin. Glycerin is a highly viscous fluid with a low frequency dielectric constant of 42.5.[6] The ratio of the device sensitivity in glycerin to the sensitivity in air at 1.0 kHz was found to be 26.5 ± 4.4. This sensitivity ratio is expected to be determined by the appropriate ratio of the depolarization coefficients N. Equation (20) predicts that N(air) : N(glycerin) is 30.0 which is in excellent agreement with the measured sensitivity ratio.

5.3 Resonant Mode Structure

Dynamic intrinsic sensitivity measurements, illustrated in Figure 7, exhibit a pronounced frequency structure. This structure has been tentatively identified as the mechanical resonances of the fiber-copolymer composite. The low frequency optical path length changes in the sensor area are primarily determined by the longitudinal strain (e_{zz}) in the optical fiber core. Therefore, it is expected that the peaks in the frequency response correspond to resonances in the e_{zz} strain.

The fiber-copolymer composite will be modeled as a glass rod of length L embedded in a plastic of length L'. The determination of the resonant mode structure of the composite will be complex. However, for the purposes of discussion presented here, the mode structure will be modeled by the characteristic frequencies of longitudinal vibrations in a glass rod

with free or fixed ends:

$$f_n^2 = \frac{E}{2\rho}\frac{n^2}{L^2}. \qquad (21)$$

Here n is an integer labelling the resonant mode, E the Young's modulus of the glass rod, ρ the density, L is the rod length, and f is frequency. We can imagine a resonant mode associated with the length of the embedded segment, L', resulting from the discontinuity in the elastic properties at the points where the fiber enters the plastic. For a detector length of 15cm, equation (21) yields a resonant frequency of 19 kHz. This suggests that the peak at 14 kHz may represent a resonance in the axial strain of the fiber core associated with the detector length. The characteristic frequency for the entire sensor arm length is 1.5 kHz. Hence, the smaller resonance appearing at 3.5 kHz may be associated with vibrations in the core extending over the entire length of the fiber. The exact characterization of the sensor frequency response requires a complete analysis of the device resonant structure.

Further evidence supporting the identification of the peaks in the frequency response with the composite resonant mode structure was obtained when the sensitivity measurements were performed in glycerin. Frequency response measurements in the glycerin bath exhibit a broadening of the major peak at 14 kHz and suggest some shift in position to a lower frequency. This behavior is characteristic of damped resonant systems and presumably arises from the effect of the highly viscous fluid on the mechanical resonances of the fiber-copolymer composite.

6.0 CONCLUSION

In conclusion, interfacing of a piezoelectric copolymer and a single mode fiber has produced a fiber optic external electric field sensor. The sensor exhibits an intrinsic sensitivity of $(0.20 \pm 0.03) \times 10^{-12}$ m/V at 1.0 kHz. A model calculation of the detector sensitivity is in agreement with these measurements, indicating a sound understanding of the transduction mechanism. The polymer material parameter that determines the maximum

sensitivity is found to be d^{eff}/N. Although PVDF has a larger d^{eff}, it may not produce a significant sensitivity improvement due to its correspondingly larger dielectric constant. The optimal fiber thickness is determined by the planar structure factor g and limitations to fiber thickness imposed by the dielectric breakdown properties (crucial during the poling phase of the fabrication procedure) of the polymer film. The structure factor increases with increasing film thickness (according to equations (16) and (19)), whereas the dielectric breakdown strength is inversely proportional to the square root of the thickness.[11] Hence, there is a trade-off between structure factor and maximum film thickness that can be successfully poled. Devices referenced in (1) through (3) have not measured the sensitivity to external electric fields due to the electrode configuration used. Hence, a direct comparison of the reported sensitivities is not meaningful. A comparison may be made by considering a capacitor plate separation (for the device described here) equal to the film thickness. This would yield an intrinsic sensitivity of 1.4×10^{-12} m/V which compares well with the intrinsic sensitivity of 1.6×10^{-12} m/V reported in reference (3). Comparison with the sensor described in references (1) and (2) is complicated by their usage of stretched polymer films.

It is useful to define a minimum detectable electric field E_{min}. A device with an intrinsic sensitivity η and a minimum detectable phase shift of Θ_{min} will have a minimum detectable field determined by

$$E_{min} = \frac{\Theta_{min}}{knL\eta} \tag{22}$$

where k is the wave vector of the propagating light. Hence, an electric field detector utilizing a 1.0 km length of fiber and a phase detector capability of 10^{-7} radians,[12] is estimated to have a minimum field detectability of 33μV/m for the intrinsic low frequency sensitivity reported here.

7.0 REFERENCES

1. E.F. Carome and K.P. Koo, in Proceedings, IEEE Ultrasonics Symposium (IEEE New York, 1980), pp. 710-712.

2. K.P. Koo and G.H. Sigel, Jr., IEEE J. Quantum Electron. QE-18, 670 (1982).

3. L.J. Donalds, W.G. French, W.C. Mitchell, R.M. Swinehard, and T. Wei, Electron. Lett. 18, 327 (1982).

4. Pennwalt Corp., King of Prussia, Pa., 19406.

5. P.D. Desouza and M.D. Mermelstein, Applied Optics 21, 4214 (1982).

6. D.E. Gray, Ed. American Institute of Physics Handbook (McGraw-Hill, New York, 1963).

7. R. Hughes and J. Jarzynski, Appl. Opt. 19, 98 (1980).

8. P. Bloomfield, Pennwalt Corp.; private communication.

9. R.G. Kepler, Ann. Rev. Phys. Chem. 29, 497 (1978).

10. H. Sussner, in Proceedings, 1979 IEEE Ultrasonics Symposium (IEEE, New York, 1979), p. 498.

11. D.G. Fink and J.M. Carrol, Eds. Standard Handbook for Electrical Engineers, Tenth Edition (McGray-Hill, New York, 1969).

12. T.G. Giallorenzi, Opt. Laser Technol. 20, 73 (1981).


DAT
FILM